Evolution, 2025, **79(3)**, 380–392
https://doi.org/10.1093/evolut/qpae170
Advance access publication 26 November 2024
Original Article

OXFORD

Extended phenotype affects somatic phenotype in spiders: web builders have lower estimated biting forces than free hunters

Corinthia R. Black[1], Jeffrey W. Shultz[2], Hannah M. Wood[1]

[1]Department Entomology, National Museum of Natural History, Smithsonian Institution, Washington, DC, United States
[2]Department of Entomology, University of Maryland, College Park, Maryland, United States

Corresponding author: Department Entomology, National Museum of Natural History, Smithsonian Institution, Washington, DC, United States.
Email: corinthiablack@gmail.com

Abstract

Reciprocal selection between extended and somatic phenotypes is an active area of investigation. Recent research on the influence of web-building on somatic evolution in spiders has produced conflicting results, with some finding no effect of web use on somatic evolution and others showing significant effects. These studies differed in focus, with the former surveying general anatomical traits and the latter concentrating on somatic systems with significant functional roles in prey capture. Here we propose and test the hypothesis that prey immobilization by webs is broadly synergistic with cheliceral biting force and that web builders have lower cheliceral forces compared to free hunters. Our analysis focused on the intercheliceral (IC) sclerite and muscles, a newly characterized system that is synapomorphic and ubiquitously distributed in spiders. Using μCT scans, we quantify IC sclerite shape and model IC muscle function. Statistical analyses show that inferred size-corrected isometric muscle force is lower in web-builders than in free hunters. No such association was found for IC sclerite shape. In the investigation of reciprocal selective effects between extended and somatic phenotypes, our results highlight the importance that these traits be functionally linked and adaptive.

Keywords: Araneae, comparative phylogenetics, computed tomography, functional morphology, morphological evolution

Introduction

The term extended phenotype refers to traits that affect the external environment at a distance from the organism that produces them (Dawkins, 1982). In its original formulation, the term encompassed only organismal adaptations, that is, heritable features that are acquired, maintained, modified, or lost due to natural selection (Dawkins, 1982, 2004). Significantly, the meaning of phenotype in common usage does not contain these restrictions and effectively encompasses all observable features of an organism, not simply those that are heritable or affected by natural selection. Consequently, the extended phenotype concept has since expanded to encompass a variety of phenomena operating at different ecological scales, such as niche construction and even community evolution (Bailey, 2012; Hunter, 2018; Laland, 2004; Odling-Smee et al., 2003; Whitham et al., 2003). One advantage of Dawkins' original formulation for studies of biomechanics and functional morphology is its focus on extended adaptive phenotypes, or extended adaptations, and thereby provides a familiar framework for exploring the consequences of extended and somatic features whose functions interact. This definition is thus favorable for addressing phenomena resulting from interactions between extended and somatic functions that may manifest as evolutionary change at phylogenetic rather than ecological time scales. Classic examples of extended adaptations include external constructions such as beaver dams or spider webs (Blamires, 2010; Dawkins, 1982). Here, we explore how an extended adaptation—"foraging webs"—can alter the evolution of functionally relevant somatic traits within a clade of organisms, the spiders.

With over 50,000 documented species and growing (World Spider Catalog, 2024), spiders are the dominant invertebrate predators in most terrestrial ecosystems. The ancestral ability to produce and manipulate silk was probably key to their ecological success and phylogenetic diversification (Bond & Opell, 1998). While all spiders use silk in some capacity (egg sacs, draglines, retreats, etc.), some produce webs for capturing prey and others are webless, active hunters. Webs expanded foraging opportunities to encompass aerial insects and likely enhanced, or at least modified, the detection, interception, and restraint of prey in comparison to webless spiders. It has been hypothesized that selective pressures on foraging traits should vary based on web use and that this should be manifested as differences between web-building and webless spiders in morphology, physiology, and sensory processing. For example, foraging webs may serve as a form of "extended cognition" (Japyassú & Laland, 2017), wherein mechanical properties of the web have enhanced or replaced aspects of neural processing responsible for sensory perception. Further, recent work indicates that neuroanatomical features associated with visual processing are simplified in web-building spiders compared to spiders that lack webs (Steinhoff et al.,

Received July 3, 2024; revisions received November 10, 2024; accepted November 22, 2024
Associate Editor: Emma Sherratt; Handling Editor: Jason Wolf

2024). Orb webs appear to serve as an outsourced acoustic sensor, allowing the spider to have a greater surface for sensing vibrations than the spider's body alone (Zhou et al., 2022). However, large-scale comparative analyses that span modern spider diversity have yielded contradictory results, with some showing statistically significant effects of web use on spider morphology (Shao et al., 2023) and others finding negligible effects (Kelly et al., 2023; Wolff et al., 2021, 2022). Significantly, such studies have focused on the evolution of somatic traits of taxonomic value rather than those identified a priori as having potential functional interactions with webs.

Here, we conduct a large-scale comparative study to address whether one aspect of foraging webs, the ability to restrain prey, has impacted evolution in a synergistic somatic feature, the chelicerae. We argue that an emphasis on function is critical to understanding how extended adaptations can alter morphologies, as morphology can be functionally redundant (Wainwright et al., 2005). If alternative foraging strategies select for differences in skeletomuscular function, it is likely to be expressed in the chelicerae—the jaw-like structures most critical to the interception, restraint, and preoral processing of prey (Figure 1). However, the functional morphology of chelicerae is largely unexplored, with recent quantitative and experimental investigations focusing on unusual and/or highly specialized systems—spitting spiders (Scytodidae: Goeleven, 2017; Suter & Stratton, 2009, 2013), woodlouse hunter spiders (Dysderidae: Řezáč et al., 2008, 2021), and trap-jaw spiders (Mecysmaucheniidae: Wood et al., 2016; Wood, 2020; Malkaridae: Kallal et al., 2021a).

Spider chelicerae comprise two segments, a distal fang and a proximal paturon (cheliceral base), connected at a strong bicondylar articulation. Fang movement is controlled by a small extensor muscle and a large flexor muscle and is limited to a single plane. In contrast, the cheliceral bases connect to the body by thin, pliable cuticle that allows a wider range of movements. The absence of distinct points of articulation at the chelicera-body joint complicates interpretation of cheliceral muscle function. Each paturon has up to nine extrinsic muscles that insert on or near its proximal margin (Firstman, 1954; Palmgren, 1978, 1980; Steinbach, 1954; Whitehead & Rempel, 1959; Wood & Parkinson, 2019). Among these, the intercheliceral (IC) system is unique. It is centrally placed, consisting of a bilateral pair of anteromedial muscles that insert together between the cheliceral bases at a distinct and morphologically diverse median sclerite (Firstman, 1954; Steinbach, 1952; Wood & Parkinson, 2019) (Figure 1). This central placement is consistent with a role in lowering the chelicerae and moving the chelicerae closer together simultaneously, likely serving as the central hinge of the chelicerae, actions that are essential to biting prey. Further, among arachnids, the IC system is synapomorphic for spiders and appears to be universally distributed within the clade, and therefore, likely important to spider cheliceral function.

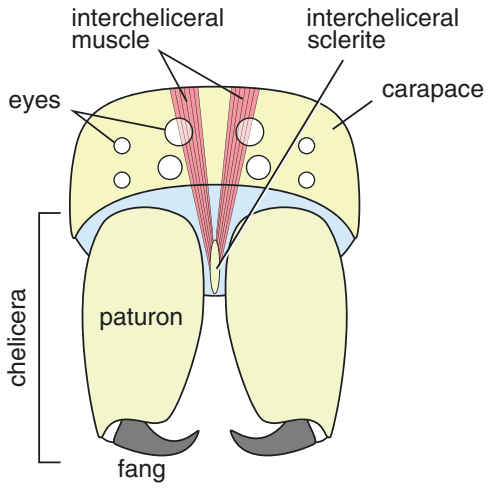

Figure 1. Anterior view of a generalized spider showing basic anatomy of the intercheliceral (IC) sclerite and muscle.

Due to functional redundancy of prey immobilization by silk and by chelicerae in web-building spiders and the absence of such redundancy in webless hunters, we hypothesize that the shape of the IC sclerite and the estimated magnitude of IC muscle forces will differ between the two ecological groups. Among spiders that utilize an extended phenotype (web-building spiders), we expect lower estimated isometric muscle forces as the mechanical properties of silk functionally replace the cheliceral bite force in prey restraint. Further, based on conclusions from Kallal and Wood (2022), we predict that free-hunting spiders will have greater disparity in function and shape of the IC system, as the chelicerae of hunting spiders may have evolved a variety of creative solutions to prey capture (e.g., variation in the degree to which legs are used in prey capture, variation in carapace/chelicerae/leg morphology), which is outsourced to the web in web-building spiders.

We tested these predictions by extracting anatomical details of the IC complex from micro-Computed Tomography (μCT) scans of 55 spider species representing a broad spectrum of phylogenetic diversity that included many web-building and webless taxa. Geometric morphometrics was used to characterize IC sclerite shape. Physiological cross-sectional area, or PCSA (a surrogate for the relative magnitude of isometric force production), was calculated by modeling the function of the IC muscles. We explored the evolution of these traits using phylogenetic comparative methods, including examination of shape space via phylomorphospace plots, evolutionary model fitting of functional and shape traits, and examination of disparity between web-builders and hunters across the major spider clades. We found that the IC muscles of spiders that use a foraging web produce lower and less disparate size-corrected isometric forces than webless hunting species. These results provide further evidence that extended adaptive phenotypes—foraging webs—influence evolution in functionally relevant skeletomuscular morphology.

Materials and methods

Computed tomography and taxon sample

In order to visualize and digitize the IC sclerite and muscle, we sampled 55 specimens representing all major spider clades for μCT (see Supplementary Table S1 for voucher information). One specimen per species was scanned with a focus on phylogenetic coverage, representing 49 of the 134 total families in spiders (~37% of spider families) and 55 genera. Intraspecies variation is minimal compared to interspecies variation, so that one specimen per species was sufficient for examining diversity in form and function and independent origins and losses of webs across the spiders. Specimens were obtained from natural history collections and had been preserved in 70%–75% ethanol. We scanned only females to

minimize effects of sexual dimorphism. Scan parameters follow Wood and Parkinson (2019; see supplemental materials). The IC sclerite was digitally labeled (segmented) using Avizo Lite version 2019.1 (Thermo Scientific, Hampton, USA) and 3D Slicer version 5.0.3 (Kikinis et al., 2014) and converted to 3D surface meshes.

Shape analysis of the intercheliceral sclerite

We used geometric morphometric techniques to capture the shape of the IC sclerite. Landmarks were placed on the IC sclerite in 3D Slicer version 5.0.3 using Slicermorph tools version e8d4a2e (Rolfe et al., 2021). Homologous landmarks were placed at the most anterior point of the sclerite and the anterior and posterior insertion points of the left and right IC muscles (Figure 2). Given the low number of homologous landmarks, five total, a high-density pseudo-landmarking protocol was modified from Fischer et al. (2022) to better capture overall shape. Twelve temporary type II landmarks were placed across the sclerite: 4 landmarks at the most extreme corners of the anterior face and 4 on the posterior face; 4 landmarks around the central portion of the sclerite, denoting the most dorsal, left lateral, right lateral, and ventral regions. All further analyses, unless otherwise noted, were performed in the R Statistical Environment version 4.4.1 (R Core Team, 2024). A spherical template with 252 vertices (landmarks) was aligned to the type II landmarks and was collapsed and patched to the 3D surfaces of each specimen in the dataset. During patching, the relax.patch option was chosen to minimize the bending energy toward the atlas. To ensure evenly spaced landmarks across the 3D meshes, surface landmarks were slid using the slider3d function in the R package Morpho version 2.12 (Schlager, 2017). To retain the surface landmarks and incorporate functionally relevant areas, the 12 type II landmarks were removed from the data set, and the 252 sliding landmarks were appended to the five homologous landmarks.

We performed a generalized Procrustes analysis to remove size, orientation, and translation using the default setting in the R package geomorph version 4.0.7 (Adams et al., 2024; Baken et al., 2021). To visualize shape variation, we performed a principal component analysis (PCA) in geomorph and determined the number of significant components using a broken-stick model in the R package PCDimension version 1.1.13 (Coombes & Wang, 2022). To visualize the shapes of the IC sclerite at the extreme ends of the PC1 and PC2 axes, a mean specimen was identified—*Trachelas tranquillus* (Trachelidae)—using findMeanSpec in geomorph and was warped to the true mean mesh of the PCA using the warpRefMesh function in geomorph. Once the true mean mesh was created, the mesh was warped to the most extreme of the PC1 and PC2 axes using warpRefMesh in geomorph.

For all comparative phylogenetic analyses that follow, the most recent and robust ultrametric phylogeny of Kallal et al. (2021b) was trimmed to match specimens in the dataset using the R package ape version 5.8 (see congeners in Supplementary Table S1) (Paradis et al., 2004). Two families in our study (Ischnothelidae, *Thelechoris*; Phyxelididae, *Ambohima*) were not included in Kallal et al., and we instead replaced them with their closest relatives (Microhexuridae, *Microhexura*, and Zodariidae, *Cybaeodamus*, respectively) based on relationships recovered from Opatova et al., 2019 and Kulkarni et al. (2023a). The resulting phylogeny was projected into multivariate shape space to generate a phylomorphospace in geomorph, which uses a maximum likelihood ancestral state estimation to determine the placement of the nodes (Adams et al., 2024; Sidlauskas, 2008).

Muscle modeling and estimation of isometric muscle force vectors

To estimate isometric forces across spiders, we established a three-dimensional Cartesian framework for the µCT scan of each specimen in 3D Slicer version 5.0.3 by setting the center

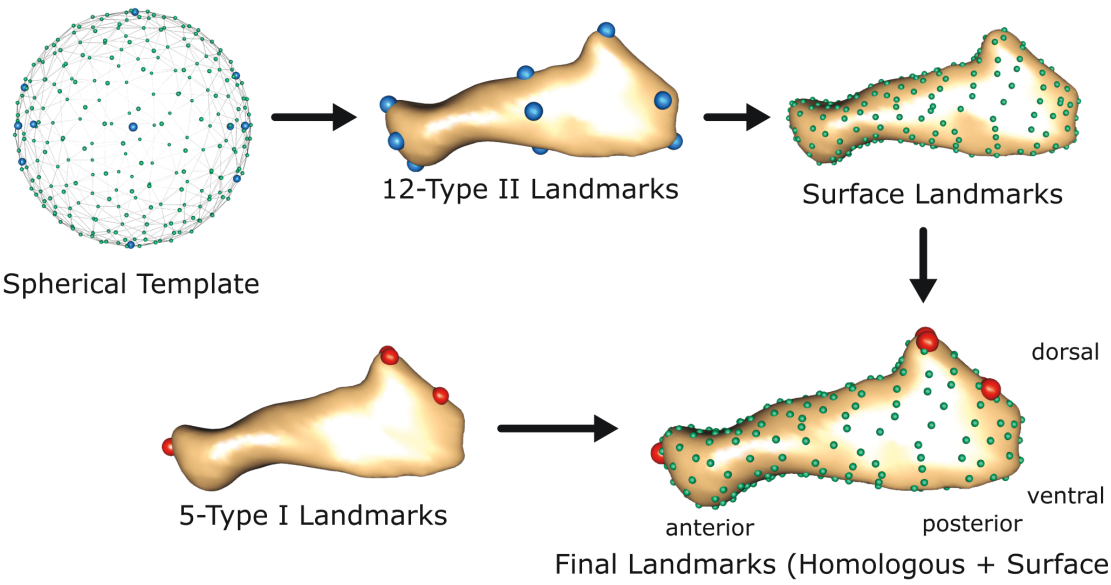

Figure 2. Example of the intercheliceral (IC) sclerite landmark scheme (*Dictyna brevitarsus*). A spherical template with 252 vertices was aligned to 12 type II landmarks, and surface landmarks were collapsed and patched to the 3D mesh. Five type I landmarks, denoting the anterior tip of the IC sclerite and the anterior and posterior edges of the left and right IC muscle attachments, were appended to the surface landmark dataset to obtain a final landmarking scheme.

of a stationary IC sclerite as the origins of the x-, y-, and z-axes (see supplemental text for definitions of axes).

The extrinsic cheliceral muscles of spiders are formed by free fibers or fascicles that pass uninterrupted from an origin on the carapace to an apodemal insertion at the cheliceral base or to the IC sclerite. This arrangement is simpler than that of most tetrapod muscles, which can be formed from multiple pennate units integrated within a tendinous complex, and estimation of PCSA is more straightforward. We modeled the left IC muscle as a system of linear virtual fibers, with each fiber originating from the center of the IC sclerite (0,0,0) and extending to a virtual horizontal section positioned just ventral to the muscle attachment site on the carapace. Given the variation in fiber number between the bilateral homologs (and possibly between individuals within the same species) and potential effects of preservational distortions, we chose the mathematical simplicity of an array of virtual fibers instead of a literal representation of the muscle. The shape of the virtual muscle section from the dorsal perspective was approximated by a four-sided polygon drawn to encompass most of the area of the actual muscle section (e.g., Figure 3A, B). This resulted in the same *z*-coordinates occurring at the end of all fibers within a specimen scan, but *z*-coordinates varied between specimens. To estimate the number of fibers within the polygon, we used the inside.owin function in the R package spatstat.geom version 3.3.2, which determines the number of observed fiber points at the longest and widest positions, estimates the number of points possible within the resulting grid system, and retains the number of points that fall within the polygon (Figure 3C, D) (Baddeley et al., 2015). The coordinates for the fiber points falling within the polygon were retained for downstream calculations and compared to the actual fiber counts using a linear model in base R to assess the accuracy of the method (R Core Team, 2024).

We determined the direction (net angle of pull) and magnitude (net isometric force) of the whole-muscle longitudinal (anterior to posterior forces), vertical (dorsal forces), and net isometric force vectors, as well as the direction of the net isometric force vector as follows: (1) *Calculate unitized fiber vectors:* Each fiber vector was assumed to contribute one unit of isometric force regardless of its length while retaining its original direction. We therefore determined the length of each fiber $(x^2 + y^2 + z^2)^{0.5}$ and divided the end coordinates and original fiber length by this value to obtain a unitized vector. (2) *Remove transverse vector component:* Due to the bilateral symmetry of the IC muscles, the transverse forces generated by simultaneous contraction were assumed to be equal and opposite. We therefore removed the transverse (x)

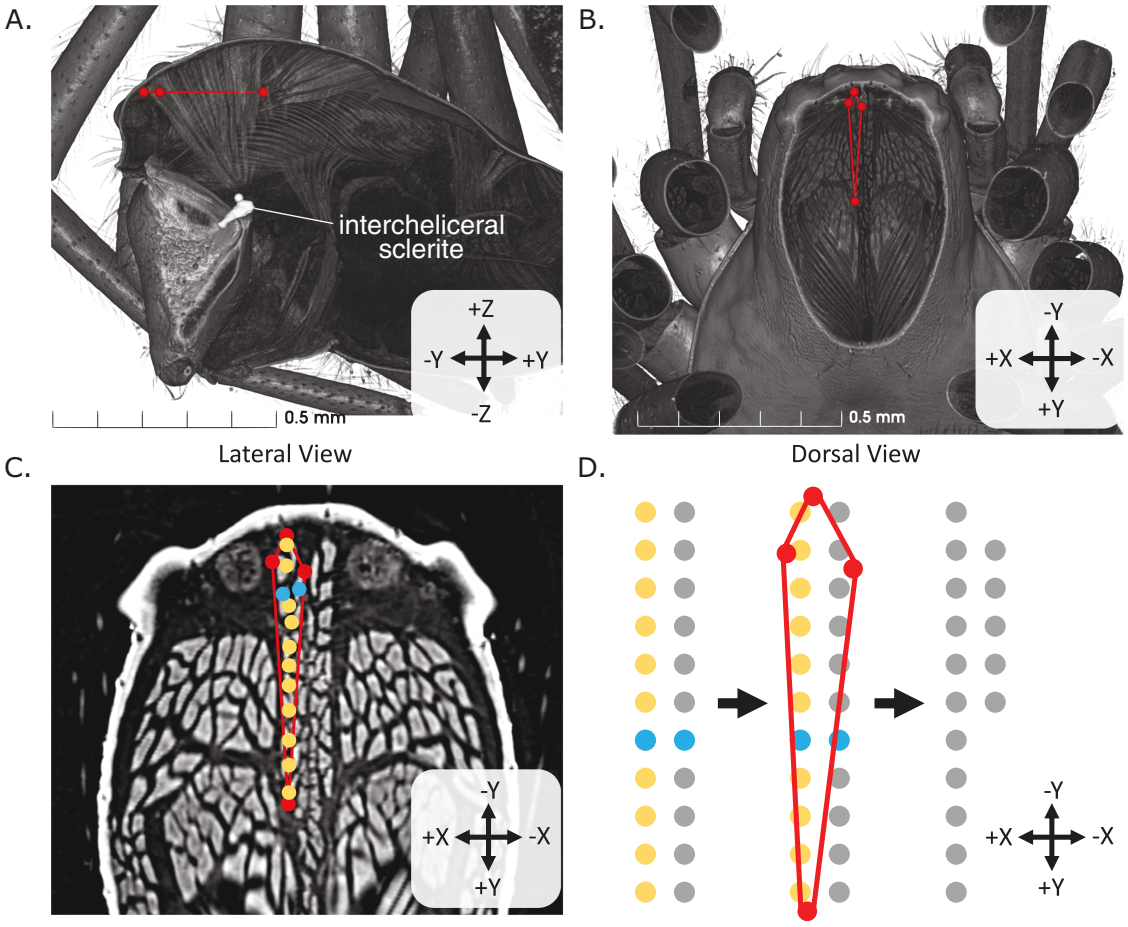

Figure 3. Methods for muscle modeling as depicted on *Dictyna brevitarsus*. Scans were aligned by rotating the images until the coxae were parallel to the *xy*-plane. (A) The coordinates at the center point of the muscle insertion (white dot) on the IC sclerite (segmented in white) were recorded, and (A, B) a polygon (red dots and lines) was placed around the left side of the IC muscle as close to the carapace as possible while retaining the same *z*-coordinates. (C) The number of fibers were recorded for the longest and widest parts of the muscle (yellow dots = longest, light blue = widest). (D) Using the number of fibers, a grid with evenly spaced points was built within the Cartesian framework. The polygon coordinates were placed within the grid, and coordinates that fell within the polygon window were retained for further muscle modeling calculations.

component of the 3D unitized vector by projecting the y and z components of the unitized vector onto the midsagittal (*yz*) plane. All subsequent calculations were performed within the midsagittal plane. (3) *Calculate magnitudes of whole-muscle longitudinal and vertical vectors:* The unitized projected y components of all fibers were summed to obtain the magnitude of the whole-muscle longitudinal vector (Y), and the corresponding z components were summed to determine the whole-muscle vertical vector (Z). (4) *Calculate the magnitude and direction of the net whole-muscle vector:* The magnitude of the net whole-muscle vector (M) was determined using $M = (Y^2 + Z^2)^{0.5}$and the direction of the corresponding angle (A) was determined using $A = \cos^{-1} Y/M$, where posterior = 0°, dorsad = 90°, and anterior = 180°. (5) *Multiply whole-muscle vectors by the force scalar*: The estimated cross-sectional area of each fiber was calculated for each species as muscle polygon area divided by the fiber number. This value was doubled to represent the combined effect of left and right muscles. The resulting value served as a force scalar. Multiplying Y, Z, and M by the scalar resulted in the relative longitudinal, vertical, and net effective isometric forces for both IC muscles contracting together. This method assumes constant sarcomere density and constant force per muscle cross-sectional area across spiders. For whole-muscle isometric forces, larger values represent stronger bite forces, whereas lower forces represent weaker bite forces. The direction of pull was based on degree, with values less than 90° representing a more posterior pull and values greater than 90° representing a more anterior pull.

Carapace width (CW) was used as the measure for size. Forces and areas of muscle attachment were size-corrected by dividing the measured value by CW raised to the isometrically appropriate exponent (i.e., CW^2). Variation remaining after size correction was assumed to reflect nonisometric effects attributable to foraging strategy, function, phylogenetic relationship, etc. The angle of net whole-muscle force and fiber number were not size corrected because isometry (geometric similarity) assumes constancy in shape. We also conducted standard regressions of natural log (ln) transformed muscle variables against ln-transformed estimates of body volume (ln CW^3) (Microsoft Excel, version 2108) to determine whether there were significant deviations from relationships expected within an isometric system. Specifically, we expected a volume exponent of 0.667 for all forces and areas and a slope of 0 or no relationship for vector angle.

Prior to PC analysis of muscle traits, each interspecific variable was standardized to a common unit using a z-score transformation. A broken-stick model was used to determine the number of components that represented the greatest amount of variation using the R package PCDimension version 1.1.13 (Coombes & Wang, 2022).

Comparative analyses

To test for correlations between IC sclerite shape and IC muscle function and the presence or absence of a foraging web, we employed phylogenetic comparative methods. For each taxon we determined whether a capture web was absent or present, scored as 0 and 1, respectively, following Kallal et al. (2021b). However, we differed from Kallal et al. in our scoring for four taxa (detailed below) because we focused less on the presence of a web and its architecture (e.g., silk-lined burrow and orb web) and instead we focused on whether the silk functioned in restraining prey. This is because a spider's web can alert the spider to prey's presence, and at the same time, the web can also physically restrain the prey. In line with our hypothesis that cheliceral function is modified when the silk does the work in capturing prey, we only scored taxa as present when it was determined that silk aided in entrapping prey. For example, *Hersilia* does not build a capture web and instead rests on a mesh of silk that serves to alert the spider to the presence of prey. Yet, *Hersilia* was still scored as present as it wraps the prey in silk by running circles around the prey prior to delivering a bite (Dippenaar-Schoeman & Jocqué, 1997). *Sphodros*, *Usofila*, and *Calileptoneta* were scored as "absent" as their silken tube or lines of silk that create a mesh or sheet likely only alert the spider to the presence of prey and do not contribute to prey restraint, based on personal communication with W. Shear and J. Ledford.

All PC axes from shape analyses and muscle modeling were used to account for total shape and function in all comparative analyses unless noted otherwise. To determine the amount of morphological disparity in IC sclerite shape and muscle variables between web-building and free-hunting spiders and within each major clade, we used the morphol.disparity function in the R package geomorph version 4.0.7 (Adams et al., 2024; Baken et al., 2021). This function measures morphological disparity of the total shape as the observed PVs within each group and performs pairwise comparisons to identify differences between groups. The Eresidae, Hypochiloidea, Nicodamoidea, and Tibial Apophysis clades were represented by one specimen each and were removed from disparity calculations. We expected disparity to be lower in web-building spiders and greater in free-hunting spiders, suggesting web-building restricts estimated bite forces to a lower value as the web constrains the prey, whereas free-hunting spiders use a variety of prey-capture techniques and would likely have higher disparity in bite forces.

Sclerite and muscle data were tested for the best-fit evolutionary model—Brownian Motion (BM), Ornstein–Uhlenbeck (OU), or Early Burst—in the R package MVmorph version 1.1.9 (Clavel et al., 2015). To test whether shape and/or muscle function showed evidence of adaptive shifts without requiring an a priori grouping, indicating multiple selective regimes where each regime has a different pattern of evolution, the PhyloEM function was used in the R package PhylogeneticEM version 1.7.0 and was set to a scalar OU model, which infers the total evolutionary rate matrix and accounts for correlations in continuous and multivariate data (Bastide et al., 2017; Law et al., 2022). Individual muscle traits were tested independently to detect differences in evolutionary model fitting. Phylogenetic signal was calculated for the total shape of the IC sclerite and for muscle variables using the R package geomorph version 4.0.7 with the K_{mult} method (Adams et al., 2024; Baken et al., 2021). This method uses a BM model to determine the degree of phylogenetic relatedness within a dataset and outputs the phylogenetic signal for all the axes combined and the contribution of each individual axis. Phylogenetic generalized least squares (PGLS) were performed to determine the correlation between the sclerite shape, muscle variables, and presence of a foraging web. To test if shape was correlated with muscle function and/or presence of a foraging web, we performed PGLS in geomorph using the procD.pgls function with generalized Procrustes analysis landmark coordinates as the response variable and foraging web presence as the predictor variable (Adams et al., 2024; Baken et al., 2021; Collyer &

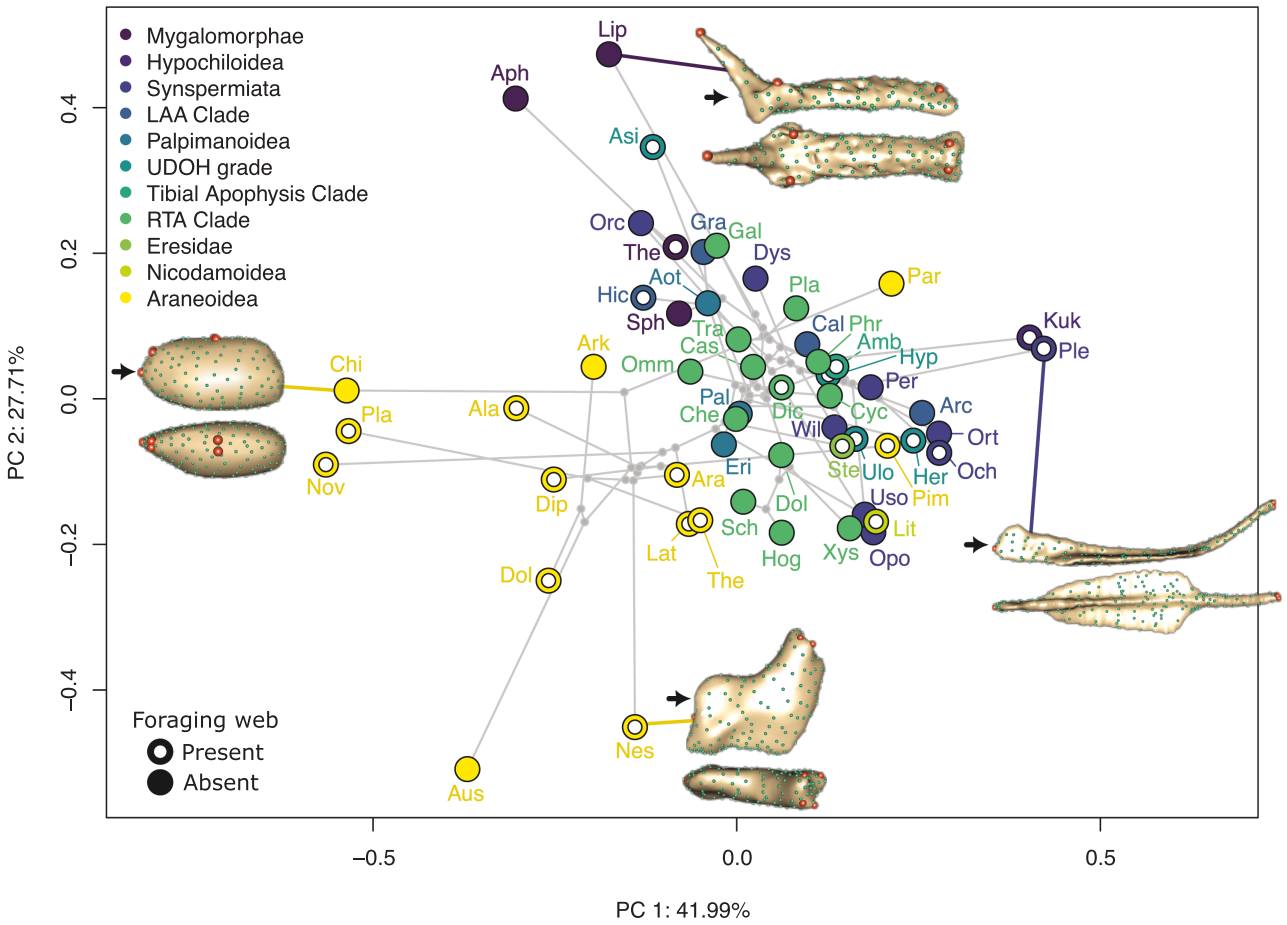

Figure 4. Phylomorphospace of IC sclerite shapes across spiders. Each point represents a single individual, and colors denote major spider clades. Gray lines connecting colored points represent phylogenetic relationships from Kallal et al. (2021b), with small gray points as the nodes of the phylogeny. Each taxon labeled by the first three letters of the genus; refer to Supplementary Table S1 for the full name. Imbedded IC sclerite shapes represent the actual shape for species at the extreme ends of the phylomorphospace; the top view is from the lateral left side of the specimen, and the bottom image is the dorsal view. Black arrows denote the anterior tip of the IC sclerite.

Adams, 2018, 2024). To test if muscle function was correlated with the presence of a foraging web, we performed PGLS in the R package nlme version 3.1.165 using the gls function with isometric forces as the response variable and foraging web presence as the predictor and the correlation option set to corBrownian to account for phylogenetic relationships (Pinheiro & Bates, 2000; Pinheiro et al., 2023). All PGLS tests used a randomized residual permutation procedure with 1,000 permutations. To visualize changes in force across the phylogeny, ancestral states were reconstructed for total force under a BM model in the R package phytools version 2.3.0 (Revell, 2024). Code and raw data are available on GitHub at github.com/corinthiablack/Pivotal-role-of-the-ICS.

Results

Shape analysis of the intercheliceral sclerite

The shape of the IC sclerite shows variability across spiders, ranging from a simple rod-like form (from long to very short) to a complex structure with various protuberances. Broken-stick analyses suggest that the first two PC axes represent the majority of shape variation, with PC1 and PC2 accounting for 41.99% and 27.71% of the total variation, respectively, and combined explaining 69.7%. Across PC1, the most extreme negative values correspond to a short and wide IC sclerite, with the muscle insertion more spread out and located closer to the anterior tip. The greatest positive values correspond to a more elongated and thinner sclerite, with the muscle insertion isolated to a single area, further from the anterior. On PC2, sclerite shape ranges from short and deep (with the muscle insertion restricted to a narrower region more dorsal to the anterior tip, on the negative end) to a longer and shallower sclerite, with the muscle insertion spread out and in line with or ventral to the anterior tip, on the positive end (Figure 4). Despite overlap between major clades within the morphospace, the araneoids trend toward the negative PC1 and PC2 quadrants (except for *Pararchaea alba* and *Pimoa laurae*), while the other clades overlap within the other quadrants (Figure 4).

Pairwise comparisons between major spider clades show that Araneoidea is significantly more disparate in IC sclerite shape than the clade containing Leptonetidae and Austrochiloidea (between-group disparity = 0.0841; $p = .0210$), the Palpimanoidea (0.0781; $p = .0460$), the RTA clade (0.0869; $p = .0010$), and the Synspermiata (0.0535; $p = .0350$). The Procrustes variance (PV) was 0.1261 in Araneoidea, which is 2.3 times larger than the average values of all the other groups. The Mygalomorphae (PV = 0.0638), Synspermiata (PV = 0.0726), and UDOH grade (PV = 0.0625) have moderate disparity, whereas the clade containing Leptonetidae and Austrochiloidea (PV = 0.0419), the Palpimanoidea

(PV = 0.0480), and the RTA clade (0.0392) have low disparity (Supplementary Table S2). The phylogenetic signal for IC sclerite shape is significantly strong ($K = 0.847$; $p = .001$), suggesting that phylogenetic relationships correlate with the shape of the IC sclerite (Supplementary Table S3).

Disparity between species that use a foraging web and those that do not use a foraging web was tested for IC sclerite shape. IC sclerite shape did not show a significant pairwise absolute difference between values ($p = .349$), and PVs for foraging web users were 0.143 compared to those that do not use a foraging web at 0.111 (Supplementary Table S2).

Muscle modeling and estimation of isometric muscle force vectors

The number of muscle fibers estimated by our method was similar to actual fiber counts with a regression slope equal to 0.9725 ($SE = 0.0162$; $p < 2^{e\text{-}16}$), with the 95% confidence intervals encompassing a slope of 1.0. This result supports the value of our approach in streamlining µCT-based estimates of PCSA. Slopes observed from linear regression of muscle force traits versus ln CW^3 (CW = size variable) were largely consistent with the expectations of an isometric system (Supplementary Table S4), with the predicted slopes of 0.667 for ln-transformed force magnitudes and 0 for total force angle falling within the 95% confidence intervals of the respective observed slopes.

The PCA of z-transformed size-corrected muscle values showed that the majority of variation in the muscle data is best represented by changes in the fiber number, fiber area, polygon area, vertical force magnitude, and total force magnitude. Broken-stick analysis suggests that IC muscle properties were best represented by two PC axes. The first axis explains 58.1% of the variation with larger fiber number counts, a larger polygon area, and higher values for the vertical and total force magnitude on the negative end of PC1 (Supplementary Figure S1). The second PC axis represented 30.3% of the variation, with changes in the longitudinal magnitude and the angle of the magnitude were seen. On the positive end of the PC2 axis, the total force vector angle is higher, whereas the force magnitudes along the longitudinal axis are higher toward the negative end (Supplementary Figure S1).

The disparity of muscle variables between major spider clades was calculated, and pairwise comparisons show that Mygalomorphae species are significantly more disparate in function than Araneoidea (between-group disparity = 6.59; $p = .004$), the clade containing Leptonetidae and Austrochiloidea (5.76; $p = .028$), the RTA clade (5.60; $p = .015$), Synspermiata (4.52; $p = .044$), and the UDOH grade (7.19; $p = .006$). Additionally, the Palpimanoidea are significantly different than the Araneoidae (8.33; $p = .004$), the clade containing Leptonetidae and Austrochiloidea (7.50; $p = .007$), the RTA clade (7.34; $p = .007$), Synspermiata (6.27; $p = .013$), and the UDOH clade (8.93; $p = .003$). The PV is 10.54 in Palpimanoidea, which is 4.54 times larger than the average of all the other groups. The Mygalomorphae (PV = 8.79), Synspermiata (PV = 4.26), RTA clade. (PV = 3.19), Leptonetidae & Austrochiloidea (PV = 3.03), and Araneoidea (PV = 2.20) have moderate disparity, whereas the UDOH grade (PV = 1.60) has low disparity (Supplementary Table S2).

Disparity between species that use a foraging web and those that do not use a foraging web was tested for IC muscle function. We found a significant difference between groups, where species that do not use a foraging web have greater disparity compared to those that use a web. The pairwise absolute difference between values was calculated to be 5.804 ($p = .001$), and the PVs for foraging webs were 3.93 compared to those that do not use a foraging web at 9.73 (Supplementary Table S2).

Phylogenetic signal is significantly strong ($K =$ or > 1) for the following traits: area of the polygon ($K = 0.9775$; $p = .004$), fiber number ($K = 1.8470$; $p = .003$), vertical force magnitude ($K = 1.018$; $p = .002$), and total force magnitude ($K = 0.9737$; $p = .001$), suggesting there is a correlation between polygon area, fiber number, and force magnitude and phylogenetic relationships. All other muscle modeling values have insignificant phylogenetic signal (Supplementary Table S3).

Comparative analyses

PhyloEM detected no shifts between BM and Ornstein–Uhlenbeck (OU) models across the phylogeny for variables associated with the IC sclerite and muscle; thus only single-regime models were considered. For shape variables, the first four axes (which represented 81.7% of the total shape) were used to test evolutionary models, as more complex models (total shape) resulted in nonconvergence, whereas the total size-corrected muscle variables were used to test evolutionary models (Supplementary Table S3). The best-fit evolutionary model for IC sclerite shape is BM, suggesting that sclerite shape evolved via random walks that resulted in increasing disparity through time. The best-fit model for polygon area, fiber number, longitudinal force, vertical force magnitude, and total force magnitude follows a BM model. The angle of the total force vector ($\theta = 95.28°C$) follows an OU model, suggesting that this trait is under stabilizing selection.

PGLS was used to determine if the overall shape of the IC sclerite correlates with IC muscle estimated isometric forces (Supplementary Table S3). The shape of the sclerite is correlated with the number of muscle fibers ($p = .015$), where a larger fiber number correlates with a more elongate sclerite, with the IC muscle insertion spread out along the sclerite. All other muscle modeling values are not significantly correlated to overall sclerite shape. In addition to muscle forces, PGLS was used to test for a correlation between shape and prey-capture method (foraging web vs. no foraging web) (Supplementary Table S3). Overall shape of the sclerite did not correlate to prey-capture method.

PGLS was also used to test for correlations between muscle function and the presence of a foraging web (Supplementary Table S3). The presence of a foraging web is correlated with a smaller polygon area of 0.0025 ± 0.0011 mm^2 ($p = .024$) and reduced muscle fiber numbers of 34.50 ± 13.20 ($p = .012$) relative to free-hunting spiders that lack foraging webs. Additionally, vertical (dorsal) force magnitude and total force magnitude of the IC muscle are correlated with the presence/absence of a foraging web. There is a decrease in IC muscle force of 0.0041 ± 0.0019 ($p = .032$) and 0.0046 ± 0.0020 ($p = .029$) in vertical magnitude and total magnitude, respectively, when a foraging web is present. No other muscle variables correlated significantly with prey-capture method.

Discussion

Presence of an extended phenotype is correlated with a shift in functional anatomy

Our original justification for predicting higher cheliceral forces in webless hunting spiders was that some of the force

required for prey restraint or immobilization is provided by silk in web-building species. This reasoning was inspired by the observation that adhesive leg scopulae are widely used for prey restraint in hunting spiders but are absent in web-builders (Wolff et al., 2013). In contrast, there is a possibility that webs act as a high-pass size filter such that the chelicerae of web-building spiders deal with smaller prey and therefore require lower cheliceral forces than webless species. This alternative is contradicted by empirical work showing that web-building spiders are capable of capturing larger prey than webless species (Nentwig & Wissel, 1986). Thus, we proposed and found support for the hypothesis that the cheliceral forces used in prey capture are generally lower in web-building spiders than in hunting spiders due to the physical properties of silk that assist in the restraint of prey.

Our examination of the skeletomuscular anatomy of spider chelicerae indicates that the intercheliceral (IC) sclerite and muscles play a significant role in cheliceral function. The medial margins of the cheliceral bases (paturons) are separated by a thin line of flexible cuticle, thus forming a loose median intercheliceral hinge. Eight of the nine pairs of extrinsic cheliceral muscles insert on the dorsal, lateral, or ventral margins of the paturon. The IC muscles are unique in attaching near the medial margins, where the bilateral pair inserts on a common median IC sclerite. This arrangement is synapomorphic for spiders, being absent in related taxa (Shultz, 1993, 1999, 2007), and appears to be distributed ubiquitously within the order. Contraction of the IC muscles appears to retract, depress, and adduct the cheliceral bases, actions that reduce intercheliceral gape, as during prey capture, and bring the chelicerae into a position suitable for feeding (maceration, extra-oral digestion, etc.). The functional conservatism of the IC muscle is reinforced further by our observation that the direction of its net effective force vector is very similar throughout the order (mean, 108°; sd, 20°) and is unaffected by body size (Supplementary Table S4). In addition, the evolution of this trait is best described by an Ornstein–Uhlenbeck (OU) model, indicating a broad-scale effect of stabilizing selection. In contrast, the evolution of the relative magnitude of estimated isometric contraction force of the IC muscles, as estimated by size-corrected PCSA, is best described by a BM model rather than an OU model, indicating that there is no order-wide tendency toward an optimal force magnitude. In fact, we found that the estimated force magnitude is lower in web-building spiders than in webless forms.

We found a significant correlation between the presence of a foraging web and a decrease in estimated IC muscle forces, but there are exceptions (Figure 5). A few taxa build webs but show relatively high forces in the IC muscle (e.g., *Novanapis*, *Stegodyphus*, and *Thelechoris*). Among web-building spiders, there are likely profound and continuous differences in the capture efficacy of different webs. For example, Araneoidea has evolved sticky silk with glue droplets that is particularly efficient at prey capture. *Novanapis* produces sticky silk and an orb web (Kulkarni et al., 2023b); however, we currently know little about prey-capture behavior. *Stegodyphus* produces a different kind of silk, cribellate, which adheres to prey via van der Waals forces and physical entanglement (Hawthorn & Opell, 2002), but likely is inferior to sticky silk (Opell & Schwend, 2009). *Thelechoris* produces neither of these silks, but observations suggest that the silk does, at least briefly, capture prey (Coyle, 1995). Thus, due to variation in the foraging web across spiders, it may only partially aid in prey capture in some lineages, which may still require high cheliceral forces to subdue prey. Here, we treated the presence of a foraging web as a discrete trait, but it is likely continuous, given the large diversity in web shape and function across spiders and the variation in the degree a web can entrap prey and/or serve as sensory input, alerting the spider to the presence of prey.

The same may be true for the webless, hunter species, which trended towards increased IC forces but showed greater levels of disparity in muscle function compared to web-building spiders. Several webless hunter species showed relatively weak forces in the IC muscle. While there is still much to learn about the behavior of many of these species, it is likely that, similar to the capture efficacy of the web, there is also continuous variation in the degree the chelicerae are used for prey capture. For example, in many webless hunting spiders, prey restraint or immobilization occurs in combination with the legs, venom, and chelicerae (Eggs et al., 2015). Spiders with foraging webs may also use their legs for grabbing and/or wrapping prey, but if the silk is primarily responsible for prey restraint, possibly to a lesser degree. It has been shown that adhesive hairs on the legs (scopulae) are common and widely distributed in the webless, active hunters (Wolff et al., 2013) but are absent in the web-building spiders, suggesting that webs and silk have functionally replaced scopulae (or vice versa) in prey capture and restraint. Thus, there is far more functional, behavioral, and morphological variation than our study captures in its limited focus on the cheliceral task of restraining prey. Further, the chelicerae are multitasking tools that are not only used for prey capture but also for a variety of other tasks (e.g., prey processing, grasping, cutting silk, and defense). The chelicerae are likely constrained by trade-offs, where optimizing for one task would occur at the expense of other tasks.

Disparity of the intercheliceral system

We found a significant difference in the disparity of muscle function between web-builders and free hunters, with greater variance and higher forces in free-hunting spiders. Among web-builders, there is significant variation in web function and architecture, suggesting that some aspects of cheliceral functional variation may have been reduced and outsourced to the foraging web. Thus, an inverse relationship may exist between web functional disparity (not tested here) and cheliceral functional disparity. Kallal & Wood (2022) did not include the IC sclerite in their study but found similar results, with the fang, paturon, and carapace shape having lower disparity in web-building spiders compared to webless spiders. Many spider lineages produce foraging webs, but in Araneoidea the evolution of sticky silk in the capture threads of the web was an important transition that is attributed to the success of this group (Coddington, 1986; Vollrath et al., 1990). Within Araneoidea, web-building has likely been lost independently in Arkyidae, Malkaridae, and Mimetidae (Kallal et al., 2021b), and these spiders have adopted an active hunter lifestyle. The high disparity observed in Araneoidea in IC sclerite shape may be due to a combination of evolving sticky silk, coupled with multiple occurrences of web loss. Our proposal that there is functional redundancy between prey restraint in foraging webs and chelicerae is supported by both the lower estimated cheliceral forces observed in web-building spiders and the lower evolutionary disparity in those forces. That selective demand for higher prey restraint

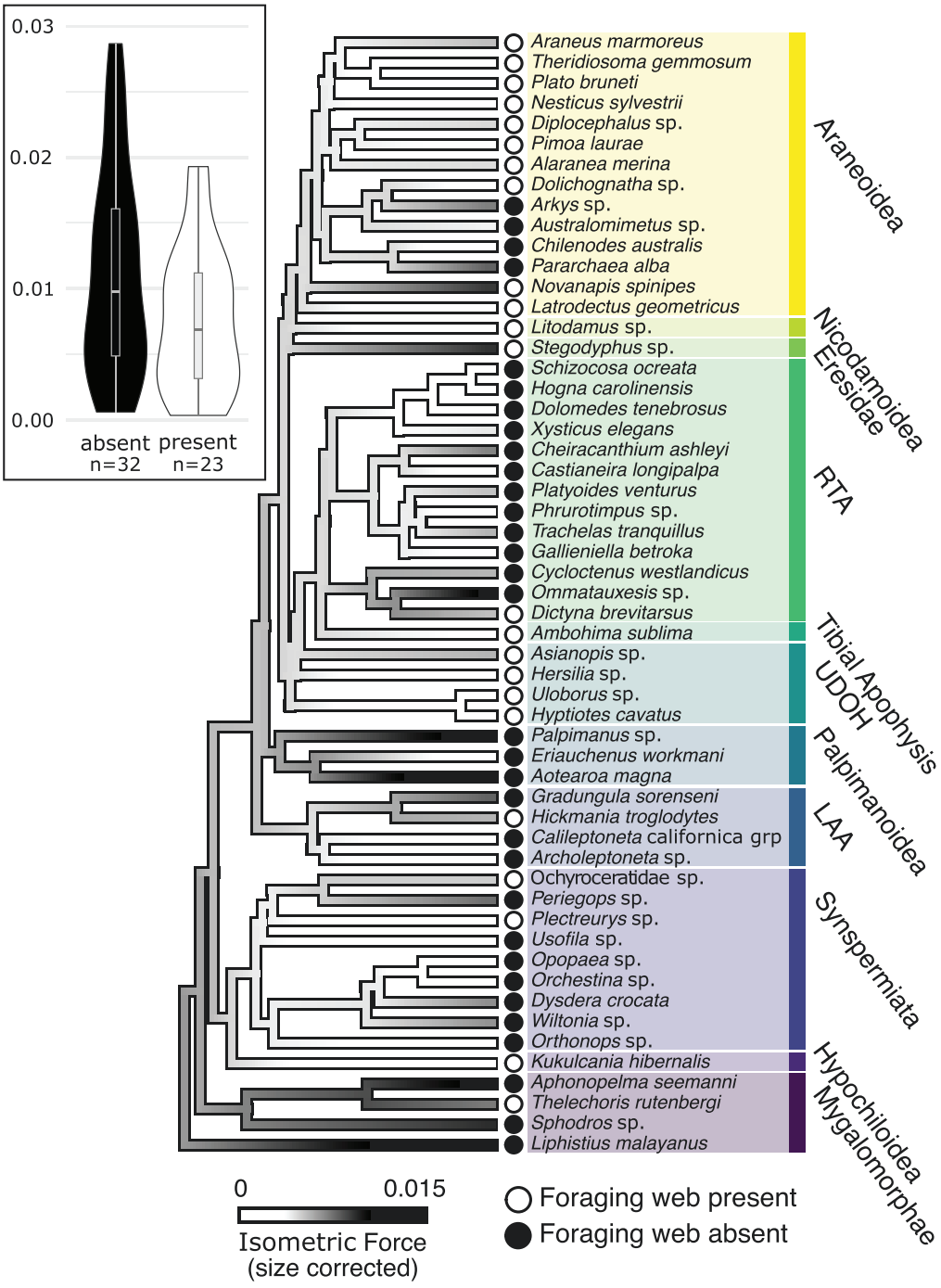

Figure 5. The total magnitude isometric force values were estimated using PCSA then size corrected and reconstructed onto the Kallal et al. (2021b) chronogram where lighter colors (white) show weaker forces whereas darker colors (black) show stronger forces. The presence or absence of a foraging web is shown at terminals, where white shows the presence of a foraging web, and black shows the absence of a foraging web. The inset violin plots show the distribution and density of total estimated isometric forces for all species with black representing the absence of a foraging web, and white representing the presence of a foraging web.

may be met by web properties in web-building spiders and by the chelicerae alone in webless hunting spiders.

Does the extended phenotype affect the evolution of somatic phenotype?

Certain groups of web-weaving spiders differ substantially in gross morphology and behavior from specific groups of free-hunting spiders. For example, the enlarged abdomens and spindly legs of many orb and cobweb spiders seem to differ from the streamlined abdomens and robust legs of most cursorial wolf spiders. But do any such differences apply broadly across spiders, and if so, can we detect these differences using phylogenetic comparative methods? The answers to these questions are interesting in themselves but can also serve as a proxy for the broader question of whether one can detect effects of extended phenotypes in the evolution of somatic phenotypes. Several attempts have been made to address this question, although the results have been mixed. We suggest

that the lack of a clear signal may reflect shortcomings of the input data rather than the basic approach.

For example, Wolff et al. (2021, 2022) approached the problem by recording 20 linear measurements of a variety of anatomical traits from a broad sample of spiders and looked for differences in the observed variation between web-building and free-hunting spiders. They detected little variation in somatic morphology that could be attributed to differences in foraging strategy; that is, few traits showed departures from order-wide tendencies. They concluded that there was no significant evidence that extended phenotypes affect the rate or direction of evolutionary change in organismal structure. The somatic traits used in these analyses were measurements commonly recorded by spider taxonomists (body size, eye width, lengths of leg segments, etc.). But the choice to rely on descriptive characters contains an assumption that foraging webs are likely to affect all or most aspects of spider morphology regardless of their potential functional interaction with webs. Otherwise, the failure to find significant associations between foraging type and morphology would have little meaning.

In contrast, in a large study of web use and somatic evolution in spiders, Shao et al. (2023) noted that some somatic traits are associated with foraging strategy. Three somatic characters (body length and two measures of the legs) were selected for analysis based on their availability in the taxonomic literature. Analysis revealed that spiders display a clade-wide tendency for body length to be either positively or inversely correlated with the relative leg length measurements. When the distribution of these traits was considered with respect to four categories of extended phenotypes (i.e., silk-lined burrows, substrate-bound webs, suspended webs, and webless), the largest spiders were found to be burrowers with relatively short legs and relatively longer patellae, and the smallest spiders were builders of suspended webs with relatively long legs and short patellae. To make sense of these results, the authors provided post hoc functional explanations for these trends (e.g., short patellae provide greater flexibility to longer legs for use in manipulating silk). However, there were no obvious morphological differences in variation expressed in spiders that build substrate-bound webs and those that build no foraging constructions. The finding that massive, short-legged spiders do not build and inhabit suspension webs and that small, long-legged spiders do not make burrows is valid but does not necessarily advance our understanding of the specific selective pressures leading to reciprocal evolution between extended and somatic phenotypes. We suggest that progress in addressing this specific issue likely depends on the formulation of hypotheses that predict functional interactions between extended and somatic phenotypes.

In summary, recent phylogeny-based comparative studies of evolutionary interactions between web use and somatic morphology were undertaken without explicit a priori interest in the functional interaction between extended and somatic adaptations. Rather, the somatic traits were quantitative features commonly measured by spider taxonomists, chosen for their taxonomic breadth, availability, or relative ease of measurement. Results of this approach are not optimal for testing whether extended and somatic adaptations are shaped by reciprocal selection. Under these analytical conditions, the finding that characters, without apparent functional relevance to web use, have no evolutionary association with web use is not necessarily surprising or informative. Nonetheless, such results have been cited as evidence for the absence of evolutionary interactions between extended and somatic features. Similarly, the discovery of apparent correlations between web use and descriptive taxonomic traits can invite post hoc functional explanations that make such associations appear obvious in retrospect. Both approaches may generate artifactual results due to p-hacking, when many characters are tested for statistical significance of association. These potential pitfalls may be reduced, although not necessarily eliminated, if somatic adaptations are chosen for their functional interaction with features of the web, whether these interactions are synergistic, redundant, complimentary, or antagonistic. The approach would be even more powerful given sufficient background information on web and somatic function that would allow the direction of the evolutionary change to be predicted, but we acknowledge such information is rarely available for clade-wide studies.

This is not to say that an approach based on function is without problems. Many adaptations have multiple functions that require the consideration of trade-offs that place limits on the direction of evolution. For example, Kelly et al. (2023) tested the hypothesis that the speeds of metabolically expensive sprints should be reduced in web-building spiders compared to webless species due to the ability of silk to restrain prey. They found no difference in sprint speeds between spiders using the two foraging strategies and concluded that the extended phenotype represented by the web had no effect on a somatic phenotype. Yet, there may be multiple roles that high sprint speed plays in spider biology, with the ability to escape from predators possibly being as critical to survival as prey capture. A similar criticism might be leveled toward our result that estimated cheliceral muscle force is lower in web-builders than in free hunters, as spiders rely on cheliceral force production for other tasks than just prey capture. Again, this highlights the value of focusing on the relative roles of extended and somatic function as implied in Dawkins' (1982) original definition of extended phenotype as extended adaptation.

Conclusions

We argue, following Dawkins (2004), that only extended adaptations should be considered in the study of extended phenotypes. We only expect a feedback loop between an extended phenotype and the organism's somatic phenotypes when these two traits are adaptive and functionally linked. The observation that phenotypic change in one somatic system can affect or be affected by phenotypic change in other somatic traits has been richly demonstrated by evolutionary and comparative research (e.g., widespread morphological and physiological impacts of changes in body size). The fact that these correlations exist does not require a change in any one somatic system to be correlated with change in all others or with change in arbitrarily selected systems. Rather, correlated change is predictable when systems are substantially linked through function, development, or some other cause. A prediction that correlated evolution should occur between leg length and lung volume in a tetrapod may be considered reasonable, whether true or not, because of their respective roles in running. Failure to find the predicted correlation may result from the absence of the assumed functional linkage or, alternatively, because one system may be more strongly linked with a competing function. This same argument can be applied to extended phenotypes; that is, when two traits, one extended and one somatic, are adaptive and functionally

linked, this provides testable hypotheses for examining the correlated evolution of somatic and "extended adaptations."

Supplementary material

Supplementary material is available online at *Evolution*.

Data availability

Raw data and code are available via GitHub: github.com/corinthiablack/Pivotal-role-of-the-ICS.

Author contributions

C.R.B.: conceptualization, methodology, formal analysis, investigation, data curation, writing—original draft, writing—review and editing, and visualization, J.W.S.: conceptualization, methodology, validation, formal analysis, writing—original draft, writing—review and editing, visualization, supervision, and funding acquisition, H.M.W.: conceptualization, methodology, validation, resources, writing—original draft, writing—review and editing, visualization, supervision, project administration, and funding acquisition.

Funding

J.W.S. was supported by the Maryland Agricultural Experiment Station. This work was supported by NSF grant DEB/IOS: 2114561, PIs H. Wood and J. Shultz.

Conflict of interest: The authors declare that they have no conflict of interest.

Acknowledgments

The majority of specimens scanned for this study were performed by HMW when supported by an NSF Postdoctoral Fellowship 1202873, to HMW, with supervision by Dula Parkinson, at the Advance Light Source synchrotron, Lawrence Berkeley National Laboratory. Additional scans were performed with the assistance of Scott Whittaker and Jennifer J. Hill at the National Museum of Natural History (NMNH, Scientific Imaging) and Tom Nguyen (NMNH, Entomology). For loan of specimens, we thank: Paula Cushing (Denver Museum of Nature and Science); Peter Jäger (Senckenberg Natural History Museum); Lauren Esposito, Chris Grinter, and Darrell Ubick (California Academy of Science). We thank Gustavo Hormiga (George Washington University) for gifts of specimens to USNM. We thank Ansie Dippenaar-Schoeman, Gustavo Hormiga, Joel Ledford, and William Shear for discussion on web evolution and spider predatory behavior. We thank J. Coddington and two anonymous reviewers for comments on the manuscript.

References

Adams, D. C., Collyer, M. L., Kaliontzopoulou, A., & Baken, E. K. (2024). *Geomorph: Software for geometric morphometric analyses. R package version 4.0.7*. https://cran.r-project.org/package=geomorph

Baddeley, A., Rubak, E., & Turner, R. (2015). *Spatial point patterns: Methodology and applications with R*. Chapman and Hall/CRC Press.

Bailey, N. W. (2012). Evolutionary models of extended phenotypes. *Trends in Ecology and Evolution*, *27*(10), 561–569. https://doi.org/10.1016/j.tree.2012.05.011

Baken, E. K., Collyer, M. L., Kaliontzopoulou, A., & Adams, D. C. (2021). geomorph v4.0 and gmShiny: Enhanced analytics and a new graphical interface for a comprehensive morphometric experience. *Methods in Ecology and Evolution*, *12*(12), 2355–2363. https://doi.org/10.1111/2041-210x.13723

Bastide, P., Mariadassou, M., & Robin, S. (2017). Detection of adaptive shifts on phylogenies by using shifted stochastic processes on a tree. *Journal of the Royal Statistical Society, Series B: Statistical Methodology*, *79*, 1067–1093.

Blamires, S. J. (2010). Plasticity in extended phenotypes: Orb web architectural responses to variations in prey parameters. *Journal of Experimental Biology*, *213*(Pt 18), 3207–3212. https://doi.org/10.1242/jeb.045583

Bond, J. E., & Opell, B. D. (1998). Testing adaptive radiation and key innovation hypotheses in spiders. *Evolution*, *52*(2), 403–414. https://doi.org/10.1111/j.1558-5646.1998.tb01641.x

Clavel, J., Escarguel, G., & Merceron, G. (2015). mvmorph: An r package for fitting multivariate evolutionary models to morphometric data. *Methods in Ecology and Evolution*, *6*(11), 1311–1319. https://doi.org/10.1111/2041-210x.12420

Coddington, J. A. (1986). The monophyletic origin of the orb web. In *Spiders webs: Behavior, function, and evolution*. William Eberhard, University of Chicago Press.

Collyer, M. L., & Adams, D. C. (2018). RRPP: An r package for fitting linear models to high-dimensional data using residual randomization. *Methods in Ecology and Evolution*, *9*(7), 1772–1779. https://doi.org/10.1111/2041-210x.13029

Collyer, M. L., & Adams, D. C. (2024). *RRPP: Linear model evaluation with randomized residuals in a permutation procedure, R package version 2.0.0*. https://CRAN.R-project.org/package=RRPP

Coombes, K. R., & Wang, M. (2022). *PCDimension: Finding the number of significant principal components*. https://cran.r-project.org/web/packages/PCDimension

Coyle, F. A. (1995). A revision of the funnelweb mygalomorph spider subfamily ischnothelinae (Araneae, Dipluridae). *Bulletin of the American Museum of Natural History*, *1*(226), 1–133.

Dawkins, R. (1982). *The extended phenotype*. Oxford University Press.

Dawkins, R. (2004). Extended phenotype – But not too extended. A reply to Laland, turner and Jablonka. *Biology and Philosophy*, *19*(3), 377–396. https://doi.org/10.1023/b:biph.0000036180.14904.96

Dippenaar-Schoeman, A. S., & Jocqué, R. (1997). *African spiders: An identification manual*. ARC Plant Protection Research Inst.

Eggs, B., Wolff, J. O., Kuhn-Nentwig, L., Gorb, S. N., & Nentwig, W. (2015). Hunting without a web: How Lycosoid spiders subdue their prey. *Ethology*, *121*, 1166–1177.

Firstman, B. L. (1954). *The central nervous system, musculature, and segmentation of the cephalothorax of a tarantula (Eurypelma californicum Ausserer)(Arachnida)*. Stanford University.

Fischer, V., Bennion, R. F., Foffa, D., MacLaren, J. A., McCurry, M. R., Melstrom, K. M., & Bardet, N. (2022). Ecological signal in the size and shape of marine Amniote teeth. *Proceedings of the Royal Society B: Biological Sciences*, *289*, 20221214.

Goeleven, D. (2017). On the spider that spits the solution of a nonsmooth oscillator. *Mathematical Biosciences*, *283*, 7–12. https://doi.org/10.1016/j.mbs.2016.11.011

Hawthorn, A. C., & Opell, B. D. (2002). Evolution of adhesive mechanisms in cribellar spider prey capture thread: Evidence for van der Waals and hygroscopic forces. *Biological Journal of the Linnean Society*, *77*(1), 1–8. https://doi.org/10.1046/j.1095-8312.2002.00099.x

Hunter, P. (2018). The revival of the extended phenotype. *EMBO Reports*, *19*(7), e46477. https://doi.org/10.15252/embr.201846477. John Wiley & Sons, Ltd.

Japyassú, H. F., & Laland, K. N. (2017). Extended spider cognition. *Animal Cognition*, *20*(3), 375–395. https://doi.org/10.1007/s10071-017-1069-7

Kallal, R. J., Elias, D. O., & Wood, H. M. (2021a). Not so fast: Strike kinematics of the Araneoid trap-jaw spider Pararchaea alba (Malkaridae: Pararchaeinae). *Integrative Organismal Biology*, *3*(1), obab027. https://doi.org/10.1093/iob/obab027

Kallal, R. J., Kulkarni, S. S., Dimitrov, D., Benavides, L. R., Arnedo, M. A., Giribet, G., & Hormiga, G. (2021b). Converging on the

orb: Denser taxon sampling elucidates spider phylogeny and new analytical methods support repeated evolution of the orb web. *Cladistics the International Journal of the Willi Hennig Society*, *37*, 298–316.

Kallal, R. J., & Wood, H. M. (2022). High-density three-dimensional morphometric analyses reveal predation-based disparity and evolutionary modularity in spider "Jaws". *Evolutionary Biology*, *49*(4), 389–402. https://doi.org/10.1007/s11692-022-09576-y

Kelly, M. B. J., Khan, M. K., Wierucka, K., Jones, B. R., Shofner, R., Derkarabetian, S., & Wolff, J. O. (2023). Dynamic evolution of locomotor performance independent of changes in extended phenotype use in spiders. *Proceedings of the Royal Society B: Biological Sciences*, *290*, 20232035. Royal Society.

Kikinis, R., Pieper, S. D., & Vosburgh, K. G. (2014). 3D slicer: A platform for subject-specific image analysis, visualization, and clinical support. In F. A. Jolesz (Ed.), *Intraoperative imaging and image-guided therapy* (pp. 277–289). Springer New York.

Kulkarni, S., Wood, H. M., & Hormiga, G. (2023a). Advances in the reconstruction of the spider tree of life: A roadmap for spider systematics and comparative studies. *Cladistics*, *39*(6), 479–532. https://doi.org/10.1111/cla.12557

Kulkarni, S., Wood, H. M., & Hormiga, G. (2023b). Phylogenomics illuminates the evolution of orb webs, respiratory systems and the biogeographic history of the world's smallest orb-weaving spiders (Araneae, Araneoidea, Symphytognathoids). *Molecular Phylogenetics and Evolution*, *186*, 107855. https://doi.org/10.1016/j.ympev.2023.107855

Laland, K. N. (2004). Extending the extended phenotype. *Biology and Philosophy*, *19*, 313–325.

Law, C. J., Blackwell, E. A., Curtis, A. A., Dickinson, E., Hartstone-Rose, A., & Santana, S. E. (2022). Decoupled evolution of the cranium and mandible in carnivoran mammals. *Evolution*, *76*, evo.14578.

Nentwig, W., & Wissel, C. (1986). A comparison of prey lengths among spiders. *Oecologia*, *68*(4), 595–600. https://doi.org/10.1007/BF00378777

Odling-Smee, F. J., Laland, K. N., & Feldman, M. W. (2003). Niche construction: The neglected process. In *Evolution (MPB-37)*. Princeton University Press.

Opatova, V., Hamilton, C. A., Hedin, M., De Oca, L. M., Král, J., Bond, J. E., & Wiegmann, B. (2019). Phylogenetic systematics and evolution of the spider infraorder mygalomorphae using genomic scale data. *Systematic Biology*, *69*(4), 671–707. https://doi.org/10.1093/sysbio/syz064

Opell, B. D., & Schwend, H. S. (2009). Adhesive efficiency of spider prey capture threads. *Zoology*, *112*(1), 16–26. https://doi.org/10.1016/j.zool.2008.04.002

Palmgren, P. (1978). On the muscular anatomy of spiders. *Acta Zoologica Fennica*, *155*, 1–41.

Palmgren, P. (1980). Some comments on the anatomy of spiders. *Annales Zoologici Fennici*, *17*, 161–173.

Paradis, E., Claude, J., & Strimmer, K. (2004). APE: Analyses of phylogenetics and evolution in R language. *Bioinformatics*, *20*(2), 289–290. https://doi.org/10.1093/bioinformatics/btg412

Pinheiro, J., & Bates, D.; R Core Team. (2023). *nlme: Linear and nonlinear mixed effects models*. https://CRAN.R-project.org/package=nlme

Pinheiro, J. C., & Bates, D. M. (2000). *Mixed-effects models in S and S-PLUS*. Springer.

R Core Team. (2024). *R: A language and environment for statistical computing*. R Foundation for Statistical Computing.

Revell, L. J. (2024). phytools 2.0: An updated R ecosystem for phylogenetic comparative methods (and other things). *PeerJ*, *12*, e16505. https://doi.org/10.7717/peerj.16505

Řezáč, M., Pekár, S., Arnedo, M., Macías-Hernández, N., & Řezáčová, V. (2021). Evolutionary insights into the eco-phenotypic diversification of Dysdera spiders in the Canary Islands. *Organisms Diversity and Evolution*, *21*(1), 79–92. https://doi.org/10.1007/s13127-020-00473-w

Řezáč, M., Pekár, S., & Lubin, Y. (2008). How oniscophagous spiders overcome woodlouse armour. *Journal of Zoology*, *275*(1), 64–71. https://doi.org/10.1111/j.1469-7998.2007.00408.x

Rolfe, S., Pieper, S., Porto, A., Diamond, K., Winchester, J., Shan, S., Kirveslahti, H., Boyer, D., Summers, A., & Maga, A. M. (2021). SlicerMorph: An open and extensible platform to retrieve, visualize and analyse 3D morphology. *Methods in Ecology and Evolution*, *12*(10), 1816–1825. https://doi.org/10.1111/2041-210x.13669

Schlager, S. (2017). Morpho and Rvcg – Shape analysis in R. P. In G. Zheng, S. Li, & G. Székely (Eds.), *Statistical shape and deformation analysis: Methods, implementation and applications*. Academic Press, an imprint of Elsevier.

Shao, L., Zhao, Z., & Li, S. (2023). Is phenotypic evolution affected by spiders' construction behaviors? *Systematic Biology*, *72*, 319–340.

Shultz, J. W. (1993). Muscular anatomy of the giant whipscorpion Mastigoproctus giganteus (Lucas) (Arachnida: Uropygi) and its evolutionary significance. *Zoological Journal of the Linnean Society*, *108*, 335–365.

Shultz, J. W. (1999). Muscular anatomy of a whipspider, Phrynus longipes (Pocock) (Arachnida: Amblypygi), and its evolutionary significance. *Zoological Journal of the Linnean Society*, *126*(1), 81–116. https://doi.org/10.1111/j.1096-3642.1999.tb00608.x

Shultz, J. W. (2007). Morphology of the prosomal endoskeleton of Scorpiones (Arachnida) and a new hypothesis for the evolution of cuticular cephalic endoskeletons in arthropods. *Arthropod Structure*, *36*(1), 77–102. https://doi.org/10.1016/j.asd.2006.08.001

Sidlauskas, B. (2008). Continuous and arrested morphological diversification in sister clades of characiform fishes: A phylomorphospace approach. *Evolution*, *62*(12), 3135–3156. https://doi.org/10.1111/j.1558-5646.2008.00519.x

Steinbach, G. (1952). Vergleichende Untersuchungen zur Chelicerenmuskulatur einiger Araneen. *Wissenschaftliche Zeitschrift der Humboldt-Universität zu Berlin*, *2*, 151.

Steinbach, G. (1954). Vergleichende Untersuchungen zu Chelicerenmuskulatur einiger Araneen. *Wissenschaftliche Zeitschrift der Humboldt-Universität Gerlin Math Naturwiss*, *2*, 1.

Steinhoff, P. O. M., Harzsch, S., & Uhl, G. (2024). Comparative neuroanatomy of the central nervous system in web-building and cursorial hunting spiders. *Journal of Comparative Neurology*, *532*, e25554.

Suter, R. B., & Stratton, G. E. (2009). Spitting performance parameters and their biomechanical implications in the spitting spider, *Scytodes thoracica*. *Journal of Insect Science*, *9*, 1–15. https://doi.org/10.1673/031.009.6201

Suter, R. B., & Stratton, G. E. (2013). Predation by spitting spiders: Elaborate venom gland, intricate delivery system. In W. Nentwig (Ed.), *Spider ecophysiology* (pp. 241–251). Springer.

Vollrath, F., Fairbrother, W. J., Williams, R. J. P., Tillinghast, E. K., Bernstein, D. T., Gallagher, K. S., & Townley, M. A. (1990). Compounds in the droplets of the orb spider's viscid spiral. *Nature*, *345*(6275), 526–528. https://doi.org/10.1038/345526a0. Nature Publishing Group.

Wainwright, P. C., Alfaro, M. E., Bolnick, D. I., & Hulsey, D. C. (2005). Many-to-one mapping of form to function: A general principle in organismal design? *Integrative and Comparative Biology*, *45*, 256–262.

Whitehead, W. F., & Rempel, J. G. (1959). A study of the musculature of the black widow spider, latrodectus mactans (fabr.). *Canadian Journal of Zoology*, *37*(6), 831–870. https://doi.org/10.1139/z59-084. NRC Research Press.

Whitham, T. G., Young, W. P., Martinsen, G. D., Gehring, C. A., Schweitzer, J. A., Shuster, S. M., Wimp, G. M., Fischer, D. G., Bailey, J. K., Lindroth, R. L., Woolbright, S., & Kuske, C. R. (2003). Community and ecosystem genetics: A consequence of the extended phenotype. *Ecology*, *84*(3), 559–573. https://doi.org/10.1890/0012-9658(2003)084[0559:caegac]2.0.co;2

Wolff, J. O., Nentwig, W., & Gorb, S. N. (2013). The great silk alternative: Multiple co-evolution of web loss and sticky hairs in

spiders. *PLoS One*, *8*(5), e62682. https://doi.org/10.1371/journal.pone.0062682

Wolff, J. O., Wierucka, K., Paterno, G. B., Coddington, J. A., Hormiga, G., Kelly, M. B. J., Herberstein, M. E., & Ramírez, M. J. (2022). Stabilized morphological evolution of spiders despite mosaic changes in foraging ecology. *Systematic Biology*, *71*(6), 1487–1503. https://doi.org/10.1093/sysbio/syac023

Wolff, J. O., Wierucka, K., Uhl, G., & Herberstein, M. E. (2021). Building behavior does not drive rates of phenotypic evolution in spiders. *Proceedings of the National Academy of Sciences of the United States of America*, *118*, e2102693118.

Wood, H., Parkinson, D., Griswold, C., Gillespie, R., & Elias, D. (2016). Extremely rapid predatory strikes evolved repeatedly in trap-jaw spiders. *Current Biology*, *26*(8), 1057–1061. https://doi.org/10.1016/j.cub.2016.02.029

Wood, H. M. (2020). Morphology and performance of the "trap-jaw" cheliceral strikes in spiders (Araneae, Mecysmaucheniidae). *Journal of Experimental Biology*, *223*, jeb.219899.

World Spider Catalog. (2024). *World spider catalog*. Version 25.5. Natural History Museum Bern. http://wsc.nmbe.ch

Wood, H. M., & Parkinson, D. Y. (2019). Comparative morphology of cheliceral muscles using high-resolution X-ray microcomputed-tomography in palpimanoid spiders (Araneae, Palpimanoidea). *Journal of Morphology*, *280*(2), 232–243. https://doi.org/10.1002/jmor.20939

Zhou, J., Lai, J., Menda, G., Stafstrom, J. A., Miles, C. I., Hoy, R. R., & Miles, R. N. (2022). Outsourced hearing in an orb-weaving spider that uses its web as an auditory sensor. *Proceedings of the National Academy of Sciences of the United States of America*, *119*, e2122789119.